



Thermobarometry and tectonic setting of the regional metamorphic rocks from South Sirjan (the Southern SSZ), Iran

Fatemeh Dehghan Nayeri ¹, Mohsen Nasrabady ^{1, *}, Mahboobeh Jamshidibadr ², Akbar Ahmadvand ³

¹ Department of Geology, Faculty of Science, Imam Khomeini International University, Iran

² Department of Geology, Faculty of Science, Payam-e-Noor University, Iran

³ Geochemistry Department, Faculty of Earth Sciences, Kharazmi University, Karaj, Iran

Received: 11 July 2023, Revised: 12 September 2023, Accepted: 23 September 2023

© University of Tehran

Abstract

There are extensive outcrops of regional metamorphic rocks that consist of marble, calcschist, metapelite, and amphibolite in the south Sirjan (southern Sanandaj-Sirjan zone). Garnet, muscovite, biotite, calcite, quartz, and feldspar are the rock-forming minerals of calcschists. Kyanite, garnet, and staurolite constitute the index minerals of the studied metapelites. Amphibole and plagioclase are the main minerals of the massive and foliated amphibolites. The *P-T* conditions of the regional metamorphic event in the southern SSZ were constrained using conventional (single-reaction) and multi-equilibrium thermobarometry (THERMOCALC software). The average temperature and pressure gained by THERMOCALC software are 8 kb, 643 °C, and 9.6 kb, 645 °C for Ky-Grt schist and calcschist samples, respectively. Using revised and recalibrated conventional thermobarometry methods result in temperature from 504 to 664 °C and pressure from 6.57 to 7.88 kb for the investigated Ky-Grt schist. Mineralogical paragenesis and thermobarometry results of the investigated metamorphic rocks are in accordance with a medium *P/T*-type metamorphic gradient. Presumably, Neotethys subduction beneath the Sanandaj-Sirjan zone and resulting crustal thickening event led to such a metamorphic gradient during Eo-cimmerian orogeny. Medium *P/T* metamorphic rocks of the southern Sanandaj-Sirjan zone and accompanying high *P/T* metamorphic rocks of the north Hajiabad could be defined as a pair of metamorphic belts that were constructed during Zagros orogeny.

Keywords: Medium *P/T* Metamorphism, Eo-Cimmerian Orogeny, Southern Sanandaj-Sirjan.

Introduction

An orogenic cycle is established with rifting events and continues while oceanic basins spread out and subduction is begun. Eventually, subduction ceased as a consequence of continent-continent or continent island-arc collision. Every one of these successive steps is characterized by distinctive tectonometamorphic events.

Most reconstructions on the closure of the Neotethys propose that the formation of the active margin along the Eurasian margin started since the Late Triassic–Early Jurassic (e.g. Berberian and King, 1981; Besse et al., 1998; Stampfli and Borel, 2002; Arvin et al., 2007). This oceanic subduction was accompanied by the formation of a cordilleran-type margin along the Sanandaj–Sirjan zone (SSZ) during Zagros orogeny in the Jurassic–Cretaceous (e.g. Berberian and Berberian, 1981; Ghasemi and Talbot, 2006) and by the formation of various marginal oceans in the back-arc domain (Inner Mesozoic Oceans of McCall, 1997).

* Corresponding author e-mail: nasrabady@sci.ikiu.ac.ir

Some geological documents of the evolutionary trend of the Zagros orogeny cycle are capable of distinguishing in the SSZ (Hassanzadeh and Wernicke, 2016; Sheikholeslami, 2016; Shakerardakani et al., 2022). However, subduction- and active continental margin- related metamorphism play a critical role in the deciphering orogeny evolution but this aspect is somewhat ignored, as most researches are largely restricted to the investigation of sedimentary facies patterns, tectono-stratigraphic evidence and magmatic events of the southern SSZ (Berberian and King, 1981; Ghasemi and Talbot, 2006; Bea et al., 2011; Alirezaei and Hassanzadeh, 2012; Sheikholeslami, 2016).

This study focuses on the mineralogy and thermobarometry of regional metamorphic rocks (Rutchun, Abshur, and Sargaz complexes) from the southern SSZ. These new data allow us to construct a geodynamic scenario of SSZ to Neotethys subduction during Eo-cimmerian orogeny.

Materials and Methods

In this contribution, we investigate mineral chemistry and thermobarometry as a tool to constrain the paleotectonic setting of regional metamorphic rocks from the south SSZ. We integrate field investigations with laboratory work through mineral chemistry. Mineral chemical compositions were obtained using a Cameca SX100 electron microprobe at the Mineral Processes Research Center, Iran (Karaj). Operating conditions were 15 kV and 15 nA beam current in full WDS mode. Mineral compositions were determined relative to natural and synthetic standards. Spot sizes varied in the 1-10 μm range, depending on the analysed phases. Mineral structural formulae were calculated through the software CalcMin_3.2 (Brandelik, 2009). Representative electron microprobe analyses (EMPA) and chemical formulas of minerals are reported in Table 1. Mineral abbreviations follow Whitney and Evans (2010).

Regional Geology

The general history of Eurasia and Gondwanaland from Permian to recent times is defined by the rifting and drifting of continental fragments from the northern margin of Gondwana land and their accretion to the southern margin of Eurasia (Hassanzadeh and Wernicke, 2016). A more subtle, early example to the west is the Cimmerian “continental ribbon,” now represented by the various continental blocks north of the main Zagros thrust (MZT). Cimmeria is generally thought to have separated from Gondwanaland in the Permian, forming the Neotethys Ocean (Sengör, 1979). Most of the debates about the formation, evolution, and ultimate closure of the Neotethys Ocean, therefore, focused on the geological details of both the ophiolites and the intervening continental elements in Iran.

The SSZ zone considered one of the Cimmerian blocks is located in the southwestern part of Central Iran and is separated from the Zagros fold-and-thrust belt by the Main Zagros reverse fault (Fig. 1a). The SSZ extends over 1500 km, from the Sabzevaran fault at its southeastern segment to as far as the Iranian-Turkish border in the northwest, with a width of 150–200 km (Fig. 1a; Moix et al., 2008). This zone largely consists of Paleozoic–Mesozoic metamorphic rocks invaded by several types of mainly Mesozoic–Cenozoic intrusions (Rachidnejad-Omran et al., 2002; Ghasemi & Talbot, 2006; Arvin et al., 2007; Sheikholeslami et al., 2008; Fazlnia et al., 2013).

The SSZ is divided at the latitude of Golpayegan into a northern and southern portion with different features (Eftekharneshad, 1981). The northern SSZ was only affected by an intra-continental rift filled with thick Triassic–Jurassic deposits (Ghasemi & Tallbot, 2006; Azizi et al., 2018; Azizi & Stern, 2019), whereas the southern SSZ was separated from central Iran along

the Nain–Baft Ocean by the Triassic onwards (Ghasemi & Tallbot, 2006; Agard et al., 2011). Both, however, were separated from the Arabian Plate by the opening of Neotethys since the Early Permian. Inversion of the oceanic basin began in the southern SSZ during the Late Jurassic–Early Cretaceous (Eo-cimmerian event), whereas in the northern part of the SSZ compressional deformation started during Cretaceous times.

Based on protolith characteristics and grade and age of metamorphism several metamorphic complexes such as Rutchun, Abshur, Sargaz, Khabr, Golgohar, and Qori are identified in the southern SSZ (Fig. 1b; c, Sabzehi et al., 1993; Sheikholeslami, 2002; Sheikholeslami et al., 2008; Fazlnia et al., 2009). These metamorphic complexes are unconformably overlain by metamorphosed to non-metamorphosed syn-orogenic turbiditic deposits of Triassic and Jurassic ages and by Jurassic volcanic rock (Nazemzadeh et al., 1996, 1997; Monsef et al., 2011; Sheikholeslami, 2015). The study area of this research is situated in the southern part of the SSZ, South of Sirjan Hajiabad (Fig. 1c), and contains outcrops of Rutchun, Abshur, and Sargaz metamorphic complexes.

Characteristics of different rock units and their stratigraphic relationships combined with evidence from magmatic and metamorphic events in the southern SSZ resulted in the identification of several tectono-stratigraphic units that record successive steps of an orogenic cycle which involved the opening and closure of the Neotethys Ocean (Sheikholeslami, 2015).

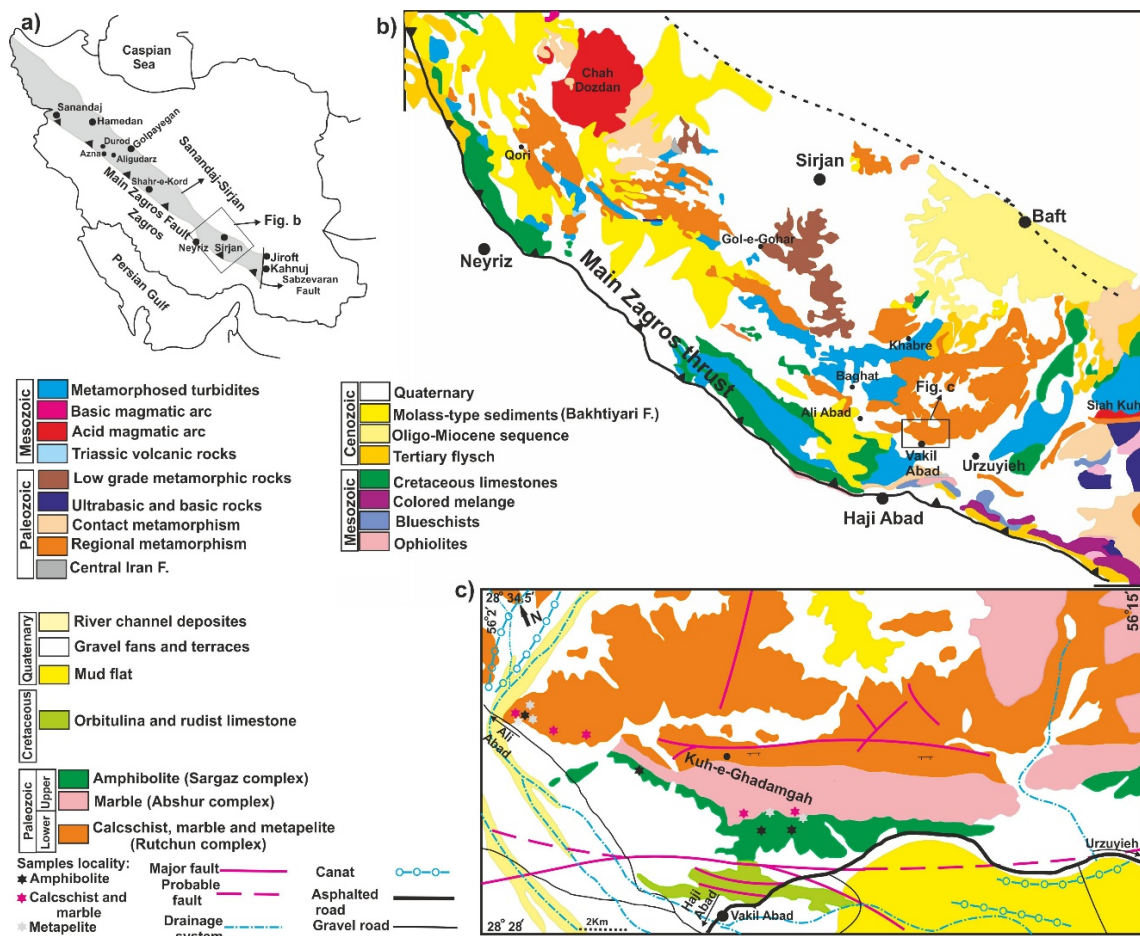


Figure 1. a- Location of the Sanandaj-Sirjan zone in Iran. b- Simplified geological map of the southern part of the Sanandaj-Sirjan zone. Modified after Hushmandzadeh et al. (1990); Sabzehei et al. (1992, 1993); and Sheikholeslami (2015). c- Simplified geological and structural map of the study area. Modified after Nazemzadeh et al., (1996, 1997)

Table 1. Continued

Mineral	Bt		Chl		Ky		St		Ep	Sph
Sample	Calcschist		Am schist	Ky-Grt schist	Ky-Grt schist		Am schist		Am schist	Am schist
Lable	Orz17		Orz7a	Orz10	Orz10		Orz7a		Orz7a	Orz7a
SiO ₂	37.45	37.13	27.93	28.03	36.27	37.21	28.28	27.11	39.52	28.8
TiO ₂	3.02	3.04	0.11	0.0	0.0	0.0	0.61	0.53	0.06	34.8
Al ₂ O ₃	17.83	18.12	19.3	20.3	62.73	62.24	53.55	55.65	26.46	3.81
FeO ^I	17.09	16.73	23.39	21.51	1.37	0.0	12.64	12.23	10.13	1.81
MnO	0.0	0.01	0.1	0.63	0.0	0.0	0.33	0.33	0.26	0.02
MgO	11.03	10.55	18.59	17.81	0.0	0.0	1.74	1.3	0.1	0.07
CaO	0.0	0.0	0.06	0.18	0.0	0.0	0.0	0.03	22.67	29.0
Na ₂ O	0.17	0.16	0.04	0.01	0.0	0.0	0.0	0.04	0.0	0.0
K ₂ O	0.17	9.49	0.01	0.0	0.0	0.0	0.0	0.01	0.0	0.0
Total	97.07	95.23	89.53	88.83	100.0	99.5	97.15	97.23	99.2	97.7
O	22	22	28	28	5	5	46	46	12.5	5
Si	5.55	5.56	5.68	5.69	0.9	0.94	7.86	7.52	3.04	0.74
Ti	0.34	0.34	0.02	0.0	0.0	0.0	0.13	0.11	0.0	0.89
Al ^{IV}	2.45	2.44	2.32	2.31	2.08	2.08	17.53	18.18	2.4	0.13
Al ^{VI}	0.66	0.76	2.31	2.57						
Fe ³⁺	0.0	0.0	0.0	0.0	0.07	0.07	0.0	0.0	0.65	0.0
Fe ²⁺	2.12	2.1	3.97	3.54	0.0	0.0	2.94	2.84	0.0	0.06
Mn	0.0	0.0	0.02	0.11	0.0	0.0	0.08	0.08	0.01	0.0
Mg	2.44	2.36	5.64	5.39	0.0	0.0	0.72	0.54	0.01	0.0
Ca	0.0	0.0	0.01	0.04	0.0	0.0	0.0	0.01	1.87	1.48
Na	0.05	0.05	0.03	0.01	0.0	0.0	0.0	0.02	0.0	0.0
K	1.98	1.81	0.01	0.15	0.0	0.0	0.0	0.0	0.0	0.0
Sum	19.58	19.42	36.01	35.91	3.05	3.03	29.25	29.29	9.01	3.31
Mg#	47	47	58	60			17	16		
Xps									21	

Field observations

There are extensive outcrops of Abshur, Sargaz, and Rutchun metamorphic complexes in the NW of Vakilabad (West Urzuyieh) that will discuss their field relations and macroscopic characteristics in this section. The general trends of these complexes are E-W and moderately dipping toward N-NW. contact boundary between these metamorphic complexes is characterized by a gradational border. Abshur complex is mainly composed of marble with intercalations of metapelites, forming the north Vakilabad Mountains (Fig. 2a). This complex is underlain by amphibolites of the Sargaz complex (Fig. 2a). These Grt-free amphibolites macroscopically show massive and foliated fabric. The felsic aggregation that composed of plagiogranite found within these amphibolites (enlarged part of Fig. 2a). Based on field documents, Sargaz amphibolites have a magmatic origin (orthoamphibolite). The Rutchun complex constructed the mountains of NW Vakilabad region. This complex mostly consists of calcschist (calcsilicate) intercalated with marble, metapelite, and Amp-schist (Fig. 2b). Spotted appearance that consists of coarse garnet that is attributed to the solution of carbonate groundmass is visible in the calcschists of Rutchun complex (Fig. 2c). Metapelite intercalations display penetrative schistosity. Garnet along with biotite porphyroblasts are visible in this unit (Fig. 2d).

Petrography

Plagioclase and amphibole are rock-forming minerals of Sargaz amphibolites (Fig. 3a).

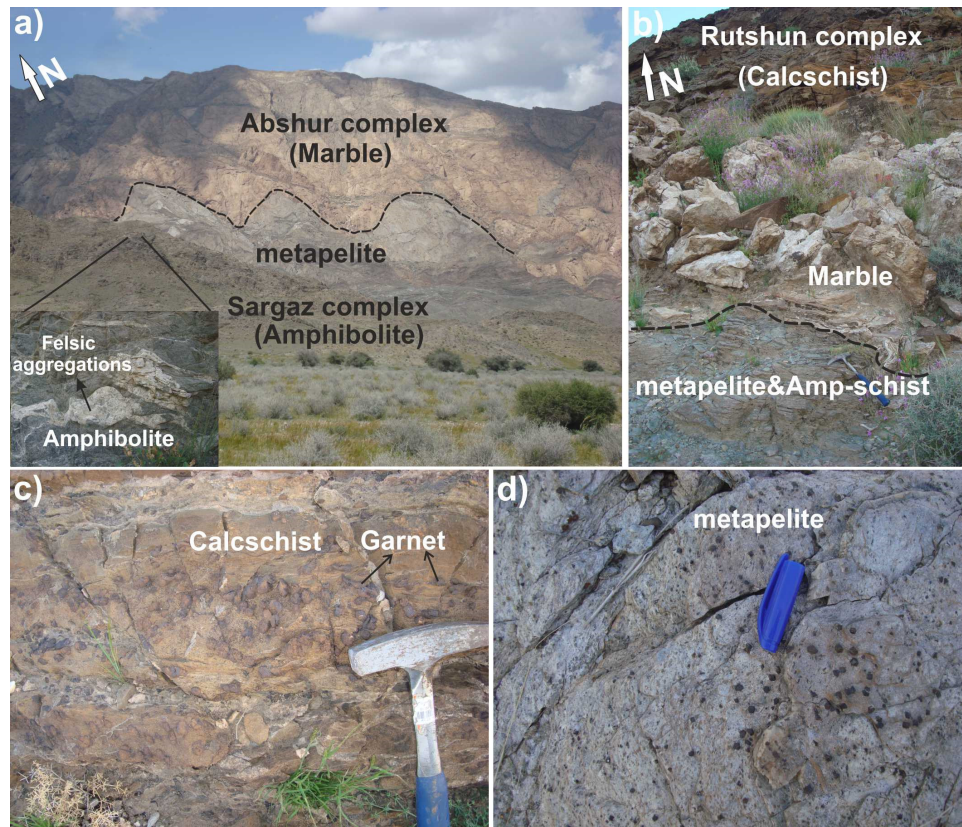


Figure 2. a- Landscape view of Abshur (marble and metapelite) and Sargaz (amphibolite) from the north of Vakilabad. b- Rutshun complex mainly consists of a calcschist that is associated with intercalations of marble, metapelite, and Amp-schist in the north of Vakilabad. c- A close-up view of the calcschist from the Rutshun complex that dot-like symbols of garnet are easy to see. d- Metapelite unite of Rutshun complex that displays garnet and biotite porphyroblasts

Accessory minerals consist of quartz, sphene, and ilmenite. Secondary biotite and chlorite are the products of amphibole breakdown. Foliated calcsilicates of the Rutshun complex contain carbonate, garnet, quartz, alkali feldspar, biotite, and muscovite as the main rock-forming minerals. Garnet and biotite developed as porphyroblast. Favorably aligned muscovite and biotite define schistosity (Fig. 3b). External schistosity is slightly wrapped around garnet porphyroblasts (Fig. 3c) indicating crystallization occurs during or prior to the development of schistosity. Crenulation foliation (S_2) is developed as a result of S_1 folding in some calcschists. Amp-schists contain the main mineral of oriented amphibole and muscovite, quartz, and feldspar (Fig. 3d). Chlorite replacing amphiboles during retrograde metamorphism. Sphene, rutile, and tourmaline are accessory minerals in the Amp-schists. Quartz, muscovite, and biotite are rock-forming minerals of metapelitic samples. Staurolite, garnet, and kyanite appeared as the index minerals (Figs. 3e, f). Schistosity is defined by aligned muscovite and biotite. Chlorite replacing biotite porphyroblasts during retrograde metamorphism. Bt-fish fabric indicating crystallization occurs prior to the schistosity development. Rutile is an important accessory mineral of schists that is partially replaced by sphene.

Mineral chemistry

Garnet

Representative garnet analyses are presented in Table 1. The investigated garnets belong to the

solid solution series of almandine (55-64%)-spessartine (4-7%)- grossular (14-32%)-pyrope (3-15%). The garnet of calcschist samples is more enriched in grossular constituents as compared to the ones of the Ky-Grt schist sample. All analyzed garnets contain more values of spessartine constituent in the core to the rim, indicating their crystallization occurs during prograde metamorphism.

Muscovite

Si cation of the investigated muscovites varies from 6.09 to 6.43. Muscovites in calcschists have lower values of Al and higher contents of Mg and Ti in comparison to ones of other samples.

Biotite

The investigated biotites have Fe# ($Fe/Fe+Mg$) ranging from 35 to 50. Biotite of calcschist samples shows more Ti contents and lesser Mg contents than one of the Ky-Grt schist samples.

Epidote

Epidotes in Amp schist have Fe^{3+} content spanning from 9.11 to 10.14%, with pistacite contents ($X_{ps} = Fe^{3+}/Al+Fe^{3+}$) ranging from 19 to 21.

Chlorite

The investigated chlorite in Amp schist and Ky-Grt schist have similar composition. They are relatively enriched in Mg with Mg# ($Mg/Fe+Mg$) varying from 58 to 60.

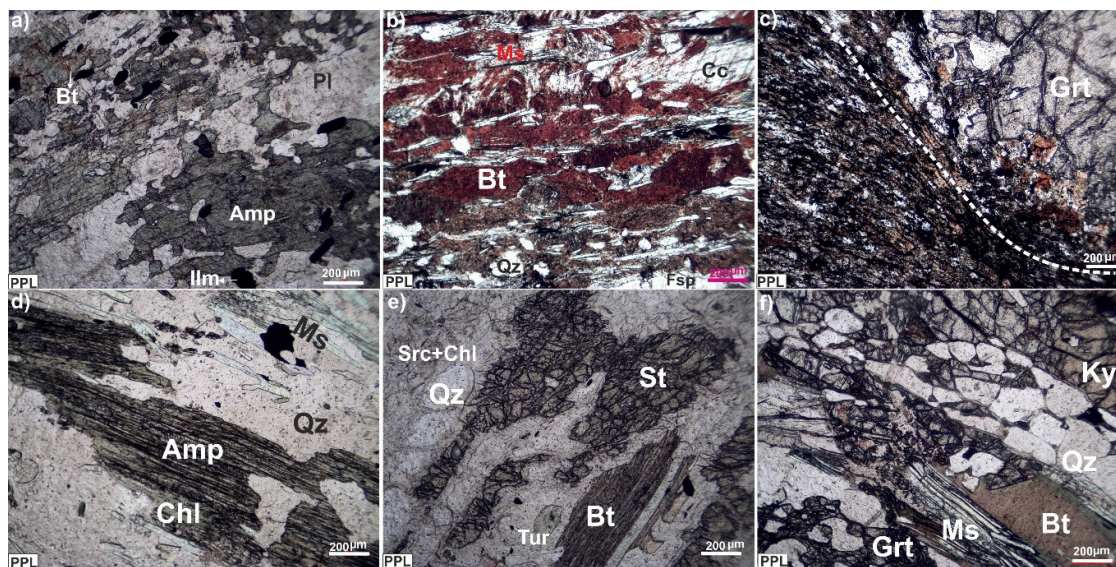


Figure 3. Mineralogy and microtexture of the studied samples at the thin section scale. a- Amphibolite with clinopyroxene and plagioclase as rock-forming minerals (Plane polarized light). b- Calcschist foliation is defined by the parallel alignment of biotite, muscovite, and calcite (Plane polarized light). c- Coarse porphyroblast of syn-to pre tectonic garnet in calcschist (Plane polarized light). d- Aligned amphibole and muscovite plus quartz are rock-forming minerals of an amphibole-schist sample (Plane polarized light). e- Staurolite schist showing biotite and quartz as a rock-forming minerals that are associated with the index minerals of staurolite. f- Kyanite-garnet schist with index minerals of kyanite and garnet

Ky-Grt schist

Microscopic observations indicate garnet, muscovite, biotite, and kyanite have been the mineral assemblage of the peak metamorphic stage in the Ky-Grt schist sample. By running THERMOCALC, this equilibrium assemblage yields average P-T conditions of 8 ± 1.9 kb and 643 ± 91 °C.

Calcschist

Garnet, calcite, muscovite, biotite, and feldspar have been considered stable paragenesis of metamorphic climax. The average P-T calculated by THERMOCALC is 9.6 ± 2.2 kb and 645 ± 45 °C.

Conventional thermobarometers

Garnet-biotite thermometry

The Fe-Mg exchange between garnet and biotite is strongly temperature dependent and therefore is widely used as a geothermometer. This geothermometer is the most widely used thermometer for estimating the T of equilibration of medium-grade pelitic metamorphic rocks (Holdaway, 2000). The cation exchange reaction can be expressed as:
$$\text{Mg}_3\text{Al}_2\text{Si}_3\text{O}_{12} + \text{KFe}_3\text{AlSi}_3\text{O}_{10}(\text{OH})_2 = \text{Fe}_3\text{Al}_2\text{Si}_3\text{O}_{12} + \text{KMg}_3\text{KAlSi}_3\text{O}_{10}(\text{OH})_2$$

Geoscientists presented more than 32 various calibrations for this thermometer (Wu and Cheng, 2006). Recalibration of mutually consistent garnet-biotite that was revised by Holdaway (2000) is one of the most valid and reliable of this kind of thermometer. Application of this calibration yields temperatures of 560 to 612 °C for the investigated Ky-Grt schist.

Garnet-muscovite thermometry

Muscovite is a ubiquitous mineral in greenschist- to amphibolite facies metapelites, thus making the garnet-muscovite (GM) geothermometer very important in determining the metamorphic P-T conditions of metapelitic rocks. According to the garnet-muscovite geothermometer that refined by Wu and Zhao (2006), the temperature estimates range from 659 to 664 °C for the investigated Ky-Grt schist.

Biotite thermometry

The concentration of Ti in biotite has long been considered to be a function primarily of changing temperature conditions in metamorphic rocks and has been suggested as a potential geothermometer (Henry et al., 2005). Wu and Cheng (2015) using more than 300 natural rutile or ilmenite-bearing metapelites, a revised Ti in biotite thermometry designed based on formulation was experimentally calibrated. Using this revised thermometry results in temperature from 504 to 536 °C for the investigated Ky-Grt schist.

Garnet-Muscovite- Al_2SiO_5 -Quartz (GMAQ) geobarometry

Wu (2018) designed six formulations for the Garnet-Muscovite- Al_2SiO_5 -Quartz (GMAQ) calibration to estimate P-T conditions of metapelites involving muscovite without plagioclase. According to this calibration, a pressure of 6.59 to 7.35 kb was obtained for the investigated Ky-Grt schist.

Garnet-Biotite-Al₂SiO₅-Quartz (GMAQ) geobarometry

Most of the popular geobarometers applicable to metapelites require chemical compositions of both garnet and plagioclase to be accurately determined. However, many metapelites are CaO deficient, so plagioclase is absent from many metapelites, and such geobarometers cannot be applied to these metapelites. All these necessitated Wu (2017) to calibrate a new geobarometer applicable to metapelitic assemblages devoid of plagioclase and, naturally, apply to the broad ranges of P–T and chemical compositions of the minerals involved. GBAQ formulation yielded pressure estimates within 6.94 to 7.22 kb for the Ky-Grt schist sample.

Garnet geobarometry

In many metapelitic assemblages, plagioclase is either CaO-deficient or even absent. In such cases, all the widely applied, well-calibrated plagioclase-related geobarometers lose their usage. Hence, Wu (2019) inferred that the net-transfer reaction including intracrystalline Fe²⁺–Ca²⁺ exchange in garnet is pressure-sensitive and thus can be calibrated as a geobarometer. Based on this geobarometer we found pressure ranges from 7.72 to 7.88 kb for metamorphic conditions of the investigated Ky-Grt schist.

According to the petrogenetic grids that are defined for metabasite compositions (Liu et al., 1996; Nagel et al., 2012), the minimum pressure for the garnet appearance is 8 kb. So, the inferred pressures derived from different barometers are in line with the absence of garnet in the investigated amphibolites.

Discussion

Eo-cimmerian orogeny is predominantly characterized by metamorphism, continental collision, and subsequent granitization in central Iran (Bagheri and Stampfli, 2008; Zanchi et al., 2009a; 2015), NE Iran (Karimpour et al., 2010; Zanchetta et al., 2013) and the western Alborz (Zanchi et al., 2009b; Razaghi et al., 2018) regions. But this orogeny has resulted in Neotethys subduction initiation and its subsequent metamorphism, magmatism, and thickening events in the active continental margin of the SSZ during the Jurassic (Wilmsen et al., 2009; Sheikholeslami, 2015; Hassanzadeh and Wernick, 2016).

SSZ represents the “core zone” or “metamorphic core” of the Arabia-Eurasia collision zone (Mohajjel and Fergusson, 2014; Hassanzadeh and Wernicke, 2016). Hence, SSZ inquiry plays a critical role in the evolution and deciphering of the Arabia-Eurasia collisional events, nevertheless, its metamorphic history is poorly known (Hassanzadeh and Wernicke, 2016). Most of the SSZ has been underwent polymetamorphic sequence that overprinted by contact metamorphism as a result of intrusion emplacement (Berberian and King, 1981; Hassanzadeh and Wernicke, 2016; Monfaredi et al., 2020; Shakerardakani et al., 2022). Furthermore, the distribution of metamorphic rocks is relatively sparse and discontinuous in this zone, and much of the metamorphism predates the Arabia-Eurasia collision by 100 My or more (Hassanzadeh and Wernicke, 2016).

The occurrence of various geodynamic conditions of the Neotethys subduction zone and its resultant diversity of continental active margin, have probably led to distinct metamorphic gradients in different pieces of the Sanandaj-Sirjan zone. The predominance of these various geodynamic conditions have also been revealed in a back-arc setting. Neotethys subduction beneath the southern SSZ resulted in the birth of the Nain-Baft back-arc basin while it is associated with an aborted rift as old as Triassic to Jurassic that was filled by sedimentary and magmatic rocks, in the northern SSZ (Ghasemi and Tallbot, 2006; Arefnia and Shahriari, 2009; Azizi et al., 2018; Azizi and Stern, 2019).

Metamorphic rocks include the widespread Late Triassic to Early Jurassic Hamadan phyllites, interpreted as back-arc deposits and considered a lateral facies variation from the Songor-Kangavar volcanic arc series (Braud and Bellon, 1974). The emplacement of Jurassic calc-alkaline intrusions like Alvand batholith into the Hamadan phyllites resulted in a contact metamorphism event encompassing Hornfels and various spotted foliated rocks, that has been followed by a low-pressure high-temperature regional metamorphism (Abukuma type metamorphism) or low *P/T* series during Cretaceous (Baharifar et al., 2004; Sepahi et al., 2004; Agard et al., 2005; Sepahi et al., 2009; Monfaredi et al., 2020).

Shakerardakani et al., (2022) reported a sequential metamorphic evolution in the central SSZ (Dorud–Azna complex) during a Wilson cycle. They proposed that the late Carboniferous high-*T*/low-*P* orogenic and late Jurassic amphibolite-grade metamorphic events of the central SSZ reflect various stages of a Wilson cycle, from rifting to subduction initiation in final plate collision.

Eclogite facies rocks as old as 184 Ma have been reported from central SSZ around the Shahr-e-Kord region (Davoudian et al., 2008, 2016). These eclogites predate approximately 100 Ma compared to Zagros blueschists (Agard et al., 2006). Alternatively, Shahr-e-Kord eclogites are associated with paragneisses while Zagros blueschists display an intimate association with serpentinites. Hence, Shahr-e-Kord eclogites have been considered the outer edge of the central Iran block that experienced tectonic erosion and ensuing subduction zone metamorphism during Neotethys subduction initiation in early Jurassic time (Fig. 5a) (Davoudian et al., 2016, Jamali Ashtianai et al., 2020).

Regional metamorphic rocks of NE Neyriz (Qori complex) consist mostly of migmatitic amphibolite, marble, and Ky schist that have undergone partial melting under conditions of medium *P/T* metamorphic gradient during Jurassic. This metamorphic episode is attributed to the Neotethys subduction-induced crustal thickening during Eo-cimmerian orogeny (Sheikholeslami et al., 2008; Fazlnia et al., 2009).

Based on thermobarometry results discussed in the previous section, the average geothermal gradient of the southern SSZ from 20 to 25 °C/km is obtained, in accordance with other metamorphic complexes from Gole Gohar (Fatehi and Ahmadipour, 2017b), Neyriz (Fazlnia et al., 2009) and Dorud-Azna (Shakerardakani et al., 2022) regions of the SSZ. Sillimanite and cordierite absence along with the occurrence of kyanite and staurolite in the investigated regional metamorphic rocks are in line with the metamorphic gradient of medium *P/T*. Such metamorphic gradients are dominant in continental collision or continental active margin environments (Bucher and Grapes, 2011). Although there is some variation, the consensus is that SSZ became an active margin associated with an accretionary prism after the Late Triassic (Mohajjel et al., 2003; Sheikholeslami et al., 2008; Agard et al., 2011; Mohajjel and Fergusson, 2014; Hassanzadeh and Wernick, 2016; Sheikholeslami, 2016).

Crustal thickening that is associated with the intrusion of mafic magma in the tectonic setting of continental active margin can elevate geotherms to temperatures high enough for medium *P/T* metamorphism to occur. Neither mafic nor intermediate-felsic intrusions are found in the study area of southern SSZ. Hence a shortening event in the continental crust was responsible for the increase in the geothermal gradient rather than magmatic activity. Therefore, the investigated medium *P/T* regional metamorphic rocks from the southern SSZ can be derived from crustal materials of a continental margin that underwent thickening as a result of Neotethys subduction underneath the Sanandaj-Sirjan zone.

The juxtaposition of blueschist facies rocks around the Hajiabad region at the rear of the Zagros suture (Agard et al., 2006; Angiboust et al., 2016; Ahmadvand et al., 2021) with the studied Barrovian- type assemblages is reminiscent of a paired metamorphic belt (Miyashiro, 1961; Brown, 2010). The high *P/T* facies series typically develops along the outer paired belt or within a trench, and the medium or low *P/T* series develop along the inner belt or magmatic arc (Fig 5b).

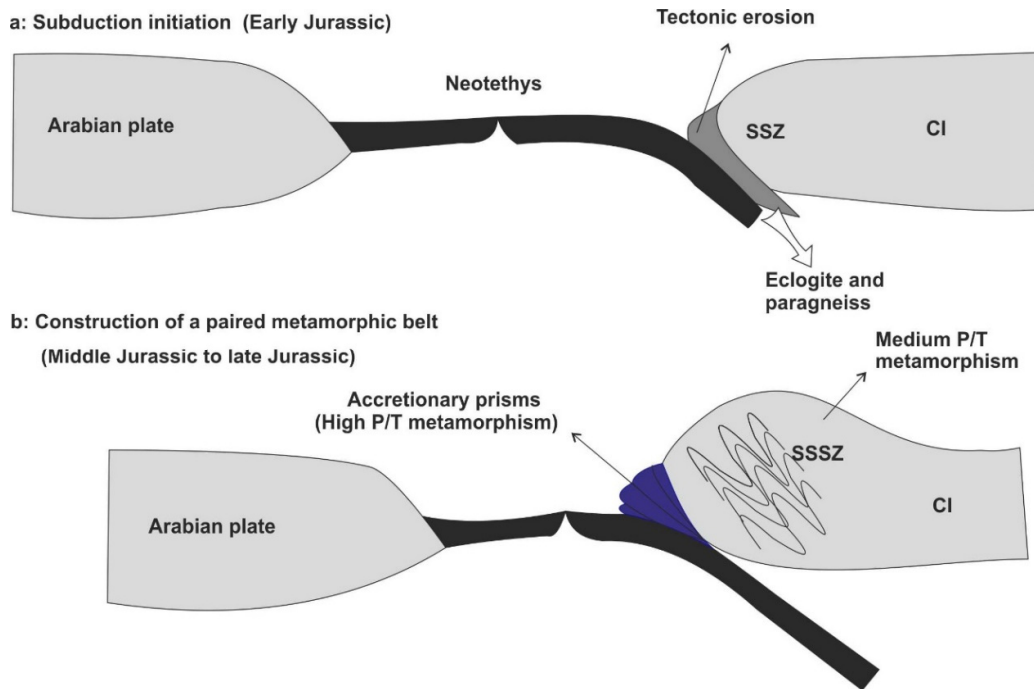


Figure 5. Schematic reconstruction of the geodynamic evolution of the SSZ during Jurassic (source of data and readapted after Agard et al., 2006, Davoudian et al., 2016; Hassanzade & Wernicke, 2016; Sheikholeslami, 2015; 2016; Jamali Ashtiani et al., 2020). (a) Subduction initiation and tectonic erosion led to the formation of Shahr-e-Kord eclogites and paragneisses. (b) Development of the high P/T (Zagros blueschists) and medium P/T (southern Sanandaj-Sirjan metamorphic rocks) facies series within trench, and along the inner belt, respectively (not to scale, location of structures is only indicative). CI: Central Iran, SSZ: Sanandaj-Sirjan, SSSZ: Southern Sanandaj-Sirjan zone

Conclusions

Based on field, mineralogy, and thermobarometry results as derived from the regional metamorphic rocks in the southern SSZ, the major outcomes of the research can be summarised as follows:

Mineralogical documents such as the occurrence of kyanite and staurolite and the absence of andalusite and cordierite in the regional metamorphic rocks from the southern SSZ are compatible with the typical medium P/T metamorphic gradient of orogenic setting.

According to the thermobarometry results, the dominant geothermal gradient has been 20 to 25 °C/km during regional metamorphism. This geothermal gradient is following pressure and temperature conditions of the tectonic setting of an active continental margin.

The investigated medium P/T regional metamorphic rocks are reminiscent of crustal material of active continental crust that has underwent Jurassic thickening event in the Neotethys subduction initiation during Eo-cimmerian orogeny.

Medium P/T regional metamorphic rocks of southern SSZ in combination with adjoining high P/T metamorphic rock, depict a typical paired metamorphic belt that developed during Zagros orogeny.

Acknowledgments

EPM analyses of this research were financially supported by Imam Khomeini International University. This research is a part of Ms thesis of the first author.

References

- Agard, P., Monié, P., Gerber, W., Omrani, J., Molinaro, M., Meyer, B., Yamato, P., 2006. Transient, synobduction exhumation of Zagros blueschists inferred from P-T, deformation, time, and kinematic constraints: implications for Neotethyan wedge dynamics. *Journal of Geophysical Research: Solid Earth* (1978-2012)111 (B11).
- Agard, P., Omrani, J., Jolivet, L., Mouthereau, F., 2005. Convergence history across Zagros (Iran): constraints from collisional and earlier deformation. *International Journal Earth Science*, 94: 401-419.
- Agard, P., Omrani, J., Jolivet, L., Whitechurch, H., Vrielynck, B., Spakman, W., Wortel, R., 2011. Zagros orogeny: a subduction-dominated process. *Geological Magazine*, 148 (5-6): 692-725.
- Ahmadvand, A., Nasrabad, M., Asiabandha, A., Gholizadeh, K., 2021. Metamorphic evolutions of high-pressure low-temperature units from ophiolitic mélange of North Soghan (NE Hajiabad, Hormozgan). *Petrological Journal*, 11(44): 29-56 (In Persian with English Abstract).
- Alirezaei, S., Hassanzadeh, J., 2012. Geochemistry and zircon geochronology of the Permian A-type Hasanrobat granite, Sanandaj-Sirjan belt: A new record of the Gondwana break-up in Iran. *Lithos*, 151: 122-134.
- Angiboust, S., Agard, P., Glodny, J., Omrani, J., Oncken, O., 2016. Zagros blueschists: Episodic underplating and long-lived cooling of a subduction zone. *Earth and Planetary Science Letters*, 443: 48-58.
- Arefnia, R., Shariari, S., 2009. Role of southeastern Sanandaj-Sirjan Zone in the tectonic evolution of Zagros Orogenic Belt, Iran. *Island Arc* 18, 555-576.
- Arvin, M., Pan, Y., Dargahi, S., Malekizade, S., Babaie, A., 2007. Petrochemistry of the Siah-Kuh granitoid stock southwest of Kerman, Iran: Implications for initiation of Neotethys subduction. *Journal of Asian Earth Sciences*, 30: 474-89.
- Azizi, H., Nouri, F., Stern, R.J., Azizi, M., Lucci, F., Asahara, Y., Zarinkoub, M.H., Chung, S.L., 2018. New evidence for Jurassic continental rifting in the northern Sanandaj Sirjan Zone, western Iran: the Ghalaylan seamount, southwest Ghorveh. *International Geology Review*, 62: 1635-57.
- Azizi, H., Stern, R.J., 2019. Jurassic igneous rocks of the central Sanandaj-Sirjan zone (Iran) mark a propagating continental rift, not a magmatic arc. *Terra Nova*, 31: 415-23.
- Bagheri, S., Stampfli, G.M., 2008. The Anarak, Jandaq and Posht-e-Badam metamorphic complexes in Central Iran: new geological data, relationships and tectonic implications. *Tectonophysics*, 451: 123-155.
- Baharifar, A.A., Moinevaziri, H., Bellon H., Piqué, A., 2004. The crystalline complexes of Hamadan (Sanandaj-Sirjan zone, western Iran): metasedimentary Mesozoic sequences affected by Late Cretaceous tectono-metamorphic and plutonic events. *Comptes Rendus Geoscience*, 336: 1443-1452.
- Bea, F.A., Mazhari, P., Montero, S., Amini, G., Ghalamghash, J., 2011. Zircon dating, Sr and Nd isotopes, and element geochemistry of the Khalifan pluton, NW Iran: Evidence for Variscan magmatism in a supposedly Cimmerian superterrane. *Journal of Asian Earth Sciences*, 40: 172-179.
- Berberian, F., Berberian, M., 1981. Tectono-plutonic episodes in Iran. In: Gupta, H.K., Delany, F.M. (Eds.), *Zagros Hindukush, Himalaya Geodynamic Evolution*. American Geophysical Union, Washington, DC, pp. 5-32.
- Berberian, M., King, G., 1981. Toward a paleogeography and tectonic evolution of Iran. *Canadian Journal of Earth Sciences*, 18: 210-265.
- Besse, J., Torcq, F., Gallet, Y., Ricou, L.E., Krystyn, L., Saidi, A., 1998. Late Permian to Late Triassic palaeomagnetic data from Iran: constraints on the migration of the Iranian block through the Tethyan Ocean and initial destruction of Pangaea. *Geophysical Journal International*, 135: 77-92.
- Brandelik, A., 2009. CALCMIN-An EXCEL™ Visual Basic application for calculating mineral structural formulae from electron microprobe analyses. *Computers and Geoscience*, 35 (7): 1540-1551
- Braud, J., Bellon, H., 1974. Donne'es nouvelles sur le domaine me'tamorphique du Zagros (zone de Sanandaj-Sirjan) au niveaude Kermanshah-Hamadan (Iran): nature a ge et interpretation des se' ries metamorphiques et des intrusions; evolution structurale. *Rapport Universite' Paris-Sud*, pp 1-20.
- Brown, M., 2010. Paired metamorphic belts revisited. *Gondwana Research*, 18: 46-59.

- Bucher, K., Grapes, R., 2011. *Petrogenesis of Metamorphic Rocks*. 8th edition, Springer-Verlag, Berlin. 419 p.
- Davoudian, A.R., Genser, J., Dachs, E., Shabaniyan, N., 2008. Petrology of eclogites from north of Shahrekord, Sanandaj-Sirjan Zone, Iran. *Mineralogy and Petrology*, 92: 393-413.
- Davoudian, A.R., Genser, J., Neubauer, F., Shabaniyan, N., 2016. ⁴⁰Ar/³⁹Ar mineral ages of eclogites from North Shahrekord in the Sanandaj- Sirjan Zone, Iran: implications for the tectonic evolution of Zagros orogen. *Gondwana Research*, 37: 216-240.
- Eftekharneshad, J., 1981. Tectonic division of Iran with respect to sedimentary basins. *Journal of Iranian Petroleum Association*, 82: 19-28 (in Persian).
- Fatehi, H., Ahmadipour, H., 2017a. Reconstruction of geological setting for the protolith of Gole-Gohar, Rutchun and Khabr metamorphic complexes (SW Baft, Kerman province). *Scientific Quarterly Journal*, 27 (105): 253-264 (In Persian with English Abstract).
- Fatehi, H., Ahmadipour, H., 2017b. Using chemical compositions of minerals in recognition of tectonometamorphic evolutions of Gole-Gohar and Rutchun metamorphic complexes (South of Baft, Kerman province). *Iranian journal of Crystallography and Mineralogy*, 25 (1): 79-94 (In Persian with English Abstract).
- Fazlnia, A., Schenk, V., Appel, P., Alizade, A., 2013. Petrology, geochemistry, and geochronology of the Chah-Bazargan gabbroic intrusions in the south Sanandaj-Sirjan zone, Neyriz, Iran. *International Journal of Earth Sciences*, 102: 1403-1426.
- Fazlnia, A.N., Schenk, V., van der Straaten, F., Mirmohammad, M., 2009. Petrology, geochemistry, and geochronology of trondhjemites from the Qori complex, Neyriz, Iran. *Lithos*, 112: 413-433.
- Ghasemi, A., and Talbot, C.J., 2006. A new tectonic scenario for the Sanandaj- Sirjan zone (Iran). *Journal of Asian Earth Sciences*, 26: 683-693.
- Hassanzadeh, J., and Wernicke, B.P., 2016. The Neotethyan Sanandaj-Sirjan zone of Iran as an archetype for passive margin-arc transitions. *Tectonics*, 35: 586-621.
- Henry, D.J., Guidotti, C.V., Thomson, J.A., 2005. The Ti-saturation surface for low-to-medium pressure metapelitic biotites: implications for geothermometry and Ti-substitution mechanisms. *American Mineralogist*, 90: 316-328.
- Holdaway, M.J., 2000. Application of new experimental and garnet Margules data to the garnet-biotite geothermometer. *American Mineralogist*, 85: 881-892.
- Hushmandzadeh, A., Soheili, M., Ohanian, T., Sahandi, M.R., Azarm, F., 1990. Explanatory Text of the Eqlid Quadrangle Map. Geological Survey of Iran Geological Quadrangle G10, scale 1:250,000.
- Jamali Ashtiani, R., Hassanzadeh, J., Schmitt, A.K., Sudo, M., Timmerman, M., Günter, C., Sobel, E., 2020. Geochronology and geochemistry of subducted Cadomian continental basement in central Iran: decompressional anatexis along the Jurassic Neotethys margin. *Gondwana Research*, 18: 354-366.
- Karimpour, M.H., Stern, C.R., Farmer, L., 2010. Zircon U-Pb geochronology, Sr-Nd isotope analyses, and petrogenetic study of Dehnow diorite and Kuhsangi granodiorite (Paleo-tethys), NE Iran. *Journal of Asian Earth Sciences*, 37: 384-393.
- Liu, J., Bohlen, S.R., Ernst, W.G., 1996. Stability of hydrous phases in subducting oceanic crust. *Earth and Planetary Science Letters*, 143: 161-171.
- McCall, G.J.H., 1997. The geotectonic history of the Makran and adjacent areas of southern Iran. *Journal of Asian Earth Sciences*, 15: 517-531.
- Miyashiro, A., 1961. Evolution of metamorphic belts. *Journal of Petrology*, 2: 277-311.
- Mohajjel, M., Fergusson, C.L., 2014. Jurassic to Cenozoic tectonics of the Zagros Orogen in northwestern Iran. *International Geology Review*, 56: 263-287.
- Mohajjel, M., Fergusson, C., Sahandi, M., 2003. Cretaceous-Tertiary convergence and continental collision, Sanandaj-Sirjan zone, western Iran. *Journal of Asian Earth Sciences*, 21(4): 397-412.
- Moix, P., Beccaletto, L., Kozur, H., Hochard, C., Rosselet, F., Stampfli, G.M., 2008. A new classification of the Turkish terranes and sutures and its implication for the paleotectonic history of the region. *Tectonophysics*, 451: 7-39.
- Monfaredi, B., Hauzenberger, C., Neubauer, F., Schulz, B., Genser, J., Shakerardakani, F., Halama, R., 2020. Deciphering the Jurassic-Cretaceous evolution of the Hamadan metamorphic complex during Neotethys subduction, western Iran. *International Journal of Earth Sciences*, 109: 2135-2168.
- Monsef, I., Rahgoshay, M., Whitechurch, H., 2011. Petrogenetic variations of the Jurassic magmatic

- sequences of Hoseinabad-Hajiabad regions in Sanandaj-Sirjan Zone (south of Iran). *Petrological Journal*, 1(4): 89-112 (in Persian with English abstract).
- Nagel, T.J., Hoffmann, E., Munker, C., 2012. Generation of Eoarchean tonalite-trondhjemite-granodiorite series from thickened mafic arc crust. *Geology*, 40(4): 375-378.
- Nazemzadeh, M., Roshan Ravan, J., Azizan, H., 1996. Geological Map of Baghat: Tehran, Geological Survey of Iran, scale 1:100,000.
- Nazemzadeh, M., Roshan Ravan, J., Azizan, H., 1997. Geological Map of Khabre: Tehran, Geological Survey of Iran, scale 1:100,000.
- Powell, R., Holland T.J.B., 2008. On thermobarometry. *Journal of Metamorphic Geology*, 26: 155-179.
- Powell, R., and Holland, T.J.B., 1994. Optimal geothermometry and geobarometry. *American Mineralogist*, 79: 120-133.
- Rachidnejad-Omran, N., Emami, M.H., Sabzehei, M., Rastad, E., Bellon, H., Piqué, A., 2002. Lithostratigraphie et histoire paléozoïque à paléocène des complexes métamorphiques de la région de Muteh, zone de Sanandaj-Sirjan (Iran méridional). *Comptes Rendus Geoscience*, 334: 1185-1191.
- Razaghi, S., Nasrabad, M., Gholizadeh, K., Davoudi, Z., 2018. Thermobarometry and tectonic setting of Gasht-e- Rudkhan metapelites, Gasht Metamorphic Complex, West of Rasht. *Scientific Quarterly Journal of Geosciences*, 27(108): 269-280 (In Persian with English Abstract).
- Sabzehei, M., 1996. An Introduction to General Geology of Metamorphic Complexes in Southern Sanandaj-Sirjan Zone: Tehran, Geological Survey of Iran, unpublished report [in Persian].
- Sabzehei, M., Berberian, M., Roshanravan, J., Azizan, H., Nazemzadeh, M., Alavi-Tehrani, N., Houchmand-Zadeh, A., Nowgole-Sadat, M.A.A., Madjidi, M., 1993. Geological Map of Hajiabad, Scale 1/250,000. Geological Survey of Iran, Tehran.
- Sabzehei, M., Roshan Ravan, J., Amini, B., Eshraghi, S.A., Alai Mahabadi, S., and Seraj, M., 1992. Geological Map of the Neyriz: Tehran, Geological Survey of Iran, scale 1/250,000.
- Sengör, A.M.C., 1979. Mid-Mesozoic closure of Permo-Triassic Tethys and its implications, *Nature*, 279: 590-593.
- Sepahi, A.A., Jafari, S.R., Mani-Kashani, S., 2009. Low-pressure migmatites from the Sanandaj-Sirjan Metamorphic Belt in the Hamedan region (Iran). *Geologica Carpathica*, 60(2): 107-119.
- Sepahi, A.A., Whitey, D.L., and Baharifar, A.A., 2004. Petrogenesis of Andalusite-Kyanite-Sillimanite veins and host rocks, Sanandaj-Sirjan metamorphic belt, Hamedan, Iran. *Journal of Metamorphic Geology*, 22: 119-134.
- Shakerardakani, F., Neubauer, F., Bernroider, M., Finger, F., Hauzenberger, C., Genser, J., Waitzinger, M., Monfaredi, B., 2022. Metamorphic stages in mountain belts during a Wilson cycle: A case study in the central Sanandaj-Sirjan zone (Zagros Mountains, Iran). *Geoscience frontiers*, 13(2): 101272.
- Sheikholeslami, M.R., 2002. Évolution Structurale et Métamorphique de la Marge Sud de la Microplaque de l'Iran Central: Les Complexes Métamorphiques de la Région de Neyriz (Zone de Sanandaj-Sirjan) [Ph.D. thesis]: Brest, France, Université de Brest, 164 p.
- Sheikholeslami, M.R., 2015. Deformations of Palaeozoic and Mesozoic rocks in southern Sirjan, Sanandaj-Sirjan zone, Iran. *Journal of Asian Earth Sciences*, 106: 130-149.
- Sheikholeslami, M.R., 2016. Tectono-stratigraphic evidence for the opening and closure of the Neotethys Ocean in the southern Sanandaj-Sirjan zone, Iran, *in* Sorkhabi, R., ed., *Tectonic Evolution, Collision, and Seismicity of Southwest Asia: In Honor of Manuel Berberian's Forty-Five Years of Research Contributions*. Geological Society of America Special Paper 525, doi:10.1130/2016.2525(09).
- Sheikholeslami, M.R., Pique, A., Mobayen, P., Sabzehei, M., Bellon, H., Hashem Emami, M., 2008. Tectono-metamorphic evolution of the Neyriz metamorphic complex, Quri-Kor-e-Sefid area (Sanandaj-Sirjan zone, SW Iran). *Journal of Asian Earth Sciences*, 31: 504-521.
- Stampfli, G.M., Borel, G.D., 2002. A plate tectonic model for the Paleozoic and Mesozoic constrained by dynamic plate boundaries and restored synthetic oceanic isochrones. *Earth and Planetary Science Letters*, 196: 17-33.
- Thompson, A.B., 1996. Fertility of crustal rocks during anatexis. *Transactions of the Royal Society of Edinburgh. Earth Sciences*, 87: 1-10.
- Whitney, D.L., and Evans, B.W., 2010. Abbreviations for names of rock-forming minerals. *American Mineralogist*, 95: 185-187.
- Wilmsen, M., Fursich, T., Seyed-Emami, K., Majidifard, M.R., Taheri, J., 2009. The Cimmerian

- Orogeny in northern Iran: tectono-stratigraphic evidence from the foreland. *Terra Nova*, 21: 211-218.
- Wu, C.M., 2017. Calibration of the garnet-biotite- Al_2SiO_5 -quartz geobarometer for metapelites. *Journal of Metamorphic Geology*, 35: 983-998.
- Wu, C.M., 2018. Metapelitic garnet-muscovite- Al_2SiO_5 -quartz (GMAQ) geothermobarometry. *Journal of Earth Science*, 29: 977-988.
- Wu, C.M., 2019. Original Calibration of a Garnet Geobarometer in Metapelite. *Minerals*, 9: 540; doi:10.3390/min9090540.
- Wu, C.M., Chen, B.H., 2006. Valid garnet-biotite (GB) geothermometry and garnet-aluminum silicate-plagioclase-quartz (GASP) geobarometry in metapelitic rocks. *Lithos*, 89: 1-23.
- Wu, C.M., Chen, H.X., 2015. Revised Ti-in-biotite geothermometer for ilmenite- or rutile-bearing crustal metapelites. *Science Bulletin*, 60: 116-121.
- Wu, C.M., Zhao, G.C., 2006. Recalibration of the garnet - muscovite (GM) geothermometer and the garnet - muscovite - plagioclase - quartz (GMPQ) geobarometer for metapelitic assemblages. *Journal of Petrology*, 47(12): 2357 - 2368
- Zanchetta, S., Berra, F., Zanchi, A., Bergomi, M., Caridroit, M., Nicora, A., Heidarzadeh, G., 2013. The record of the Late Paleozoic active margin of the Paleotethys in NE Iran: Constraints on the Cimmerian orogeny. *Gondwana Research*, 24: 1237-1266.
- Zanchi, A., Malaspina, N., Zanchetta, S., Berra, F., Benciolini, L., Bergomi, M., Cavallo, A., Javadi, H.R., Kouhpeyma, M., 2015. The Cimmerian accretionary wedge of Anarak, Central Iran. *Journal of Asian Earth Sciences*, 102: 45-72.
- Zanchi, A., Zanchetta, S., Berra, F., Mattei, M., Garzanti, E., Molyneux, S., 2009b. The Eo-cimmerian (Late? Triassic) orogeny in North Iran. In: *South Caspian to Central Iran basins* (Eds. Brunet, M.F., Wilmsen, M. and Granath, J. W.) Special Publications, Geological Society, London, 312: 31-55.
- Zanchi, A., Zanchetta, S., Garzanti, E., Balini, M., Berra, F., Mattei, M., Muttoni, G., 2009a. The Cimmerian evolution of the Nakhlak-Anarak area, Central Iran, and its bearing for the reconstruction of the history of the Eurasian margin. In: *Brunet, M.F., Wilmsen, M., Granath, J.W. (Eds.), South Caspian to Central Iran Basins*. Geological Society of London Special Publications, 312: 261-286.

